Mon. Not. R. Astron. Soc. **398,** 357–367 (2009) doi:10.1111/j.1365-2966.2009.15144.x

Applying laboratory thermal desorption data in an interstellar context: sublimation of methanol thin films★

Simon D. Green,[1] Amandeep S. Bolina,[2] Rui Chen,[3] Mark P. Collings,[1]† Wendy A. Brown[2] and Martin R. S. McCoustra[1]

[1]*School of Engineering and Physical Sciences, Heriot-Watt University, Edinburgh EH14 4AS*
[2]*Department of Chemistry, University College London, 20 Gordon Street, London WC1H 0AJ*
[3]*Address at time of contribution to this work: School of Chemistry, University of Nottingham, University Park, Nottingham NG7 2RD*

Accepted 2009 May 26. Received 2009 April 23; in original form 2008 December 2

ABSTRACT

Methods by which experimental measurements of thermal desorption can be applied in astrophysical environments have been developed, using the sublimation of solid methanol as an example. The temperature programmed desorption of methanol from graphitic, amorphous silica and polycrystalline gold substrates was compared, with the kinetic parameters of desorption extracted by either a leading edge analysis or by fitting using a stochastic integration method. At low coverages, the desorption shows a substrate-dependent fractional order. However, at higher coverages methanol desorption is zeroth order with kinetic parameters independent of substrate. Using a kinetic model based on the stochastic integration analyses, desorption under astrophysically relevant conditions can be simulated. We find that the chemical and morphological nature of the substrate has relatively little impact on the desorption temperature of solid methanol, and that the substrate independent zeroth-order kinetics can provide a satisfactory model for desorption in astrophysical environments. Uncertainties in the heating rate and the distribution of grain sizes will have the largest influence on the range of desorption temperature. These conclusions are likely to be generally applicable to all species in dust grain ice mantles.

Key words: astrochemistry – molecular data – molecular processes – methods: laboratory – ISM: molecules.

1 INTRODUCTION

Thermal desorption is one of several mechanisms by which molecules that have been frozen out on the surface of an interstellar dust grain, or reactively formed within the accreted ice mantle, can be returned to the gas phase (Roberts et al. 2007). In regions of star formation, where dust grains are close enough to a protostar to be warmed, this thermal mechanism may dominate the desorption of ice mantles (Markwick et al. 2002). Viti and co-workers (Viti & Williams 1999; Viti et al. 2004) have demonstrated that although the time taken for the pre-stellar core to warm from its initial temperature to beyond that at which the ice mantles have completely sublimed is relatively short on astrophysical time scales, the desorption cannot be treated as instantaneous within astrochemical models. Therefore, inclusion of thermal desorption processes in chemical models of such regions is necessary if we are to elucidate the roles played by molecules in the physics and chemistry of star formation. The difficulties in combining grain surface processes with gas phase chemical models are well known (Herbst & Shematovich 2003), and therefore simplifications and assumptions must inevitably be made. However, the validity of these assumptions can only be assured by developing a thorough understanding of the physicochemical processes occurring in the grain mantle. Such an understanding can be obtained through laboratory experimentation.

Because of its relative simplicity as a technique, temperature programmed desorption (TPD) has always been a mainstay of the field of surface science (King 1975). TPD studies of astrophysically relevant systems have been published in the surface science and chemical physics literature for many years. More recently, thermal desorption studies by numerous research groups that specifically address astrophysical questions have also appeared in the astrophysics literature (for example Acharyya et al. 2007; Gálvez et al. 2007). No laboratory experiment can exactly reproduce the conditions of thermal desorption from an interstellar dust grain, particularly with regard to the rate of heating. Other parameters, such as the deposition temperature, and the chemical composition and morphology of the dust grain mimic may also vary between experiments. Various research groups have performed experiments using differing

★In memory of Rui Chen.

†E-mail: m.p.collings@hw.ac.uk

techniques under differing conditions, producing a range of, and at times contradictory, results. In this paper, we have examined some of the issues regarding the application of laboratory thermal desorption experiments to astrophysical environments using new data, and some previously published results (Bolina, Wolff & Brown 2005, hereafter BWB05), for the desorption of solid methanol (CH_3OH).

Methanol is observed as a common component of molecular ices along many lines of sight towards molecularly rich regions (for example Dartois et al. 1999; Pontoppidan et al. 2003; Pontoppidan, van Dishoeck & Dartois 2004). Typically characterized observationally by its 3.53 μm (CH_3 symmetric stretch) band, methanol is hypothesized to be formed in grain mantles via the hydrogenation of carbon monoxide on grain surfaces (Tielens & Whittet 1997; Watanabe & Kouchi 2008). Consequently, methanol, after water and carbon monoxide, is commonly the next most abundant component of molecular ices. Indeed in some lines of sight, observations suggest that methanol may have an abundance of up to 0.25 relative to water (Pontoppidan et al. 2004). Although methanol is not likely to exist as a pure solid in astrophysical environments, understanding its behaviour is an essential step towards predicting the behaviour of icy mantles. Several experimental studies of the thermal desorption of solid methanol in an astrophysical context have been published (Sandford & Allamandola 1993; Collings et al. 2004; BWB05). Furthermore, desorption from codeposited mixtures and layered deposits of water and methanol (Collings et al. 2004; Brown et al. 2006; Wolff, Carlstedt & Brown 2007; Bahr, Toubin & Kempter 2008) and carbon dioxide and methanol (Maté et al. 2009) have also been studied. Since methanol is also an industrially important species and can be condensed at temperatures attainable with conventional liquid nitrogen cooling, there are numerous examples where its desorption from multilayers deposited on single crystal metal and metal oxide surfaces appear in the surface science literature (Sexton 1981; Christmann & Demuth 1982, Rendulic & Sexton 1982; Sexton, Rendulic & Hughes 1982, Hrbek, dePaola & Hoffmann 1984; Sexton & Hughes 1984, Attard et al. 1989; Peremans et al. 1990, 1994; Zhang & Gellman 1991; Wu, Truong & Goodman 1993; Harris et al. 1995; Jenniskens et al. 1996; Nishimura, Gibbons & Tro 1998; Günster et al. 2000; Pratt, Escott & King 2003). Here, we have combined the work of two independent research groups, studying TPD of solid methanol from graphitic, silica and gold surfaces in three separate experimental apparatus, with varied deposition temperatures and heating rates. We compare the analysis of TPD data by direct leading edge analysis with fitting using a stochastic integration package.

2 EXPERIMENTAL

Experiments were performed in three separate ultrahigh vacuum (UHV) chambers at either Heriot-Watt University (HWU) or University College London (UCL). Methanol (Fischer, research grade – HWU or BDH, 99.9 per cent – UCL) was subjected to multiple freeze-pump-thaw cycles to remove impurities prior to use.

Chamber 1, which was located at UCL, has been described in detail elsewhere (Bolina 2005; BWB05). This is a turbomolecular and ionization pumped UHV chamber with a base pressure of 2×10^{-10} mbar. The highly oriented pyrolitic graphite (HOPG) sample was mounted on a liquid nitrogen cold finger, which allowed cooling to a temperature of 89 K. Methanol was deposited by backfilling the chamber to pressures of up to 1×10^{-7} mbar. The sample was heated resistively by W-Re wires. The temperature was measured by an N-type (Nicrosil-Nisil) thermocouple wedged between the sample and the mounting plates. TPD was performed with a linear heating ramp of $0.5\,\mathrm{K\,s^{-1}}$.

Chamber 2, which was located at HWU, has also been described in detail elsewhere (Fraser, Collings & McCoustra 2002), although some changes have recently been made. It remains a diffusion pumped UHV chamber with a base pressure of 1×10^{-10} mbar. The sample was an oxygen free high conductivity copper block, which was coated by films of either polycrystalline gold or amorphous silica. This sample was mounted on a cold finger which was cooled by a closed cycle helium cryostat, and during the experiments reported here reached a base temperature of 18 K. Methanol was deposited from an effusive doser directed at the sample surface from a distance of roughly 40 mm. Deposition was measured by a pre-calibrated quartz crystal microbalance (QCM). The sample was heated by a cartridge heater inserted into a cavity in the sample block. TPD was performed with variable heating rates, with temperature measured by a KP-type (Au-Chromel) thermocouple wedged under mounting screws at the corner of the sample. With the gold substrate, the liquid nitrogen cooled line-of-sight mass spectrometer was mounted in its original angled configuration (Fraser et al. 2002). With the silica substrate, it was mounted in a horizontal configuration, with slightly improved sensitivity.

Chamber 3, which was located at HWU, has been described in detail elsewhere (Oakes 1994; Thrower et al. 2009). It is a diffusion pumped UHV chamber with a base pressure of 2×10^{-10} mbar. The silica coated stainless steel substrate was mounted on a liquid nitrogen cooled cold finger, which allowed cooling to a temperature of 118 K. Methanol was deposited by backfilling the chamber to pressures of up to 5×10^{-7} mbar. Deposition was calculated by simple collision theory (Woodruff & Delcher 1994), assuming a sticking probability of unity. The sample was heated resistively by tantalum wires. The temperature was measured by a K-type (Chromel-Alumel) thermocouple spot welded to the side of the substrate. TPD was performed at a constant heating rate of $0.1\,\mathrm{K\,s^{-1}}$.

Silica (SiO_2) was deposited onto sample substrates in a separate high vacuum chamber at HWU, by electron beam evaporation of the bulk material. A film thickness of roughly 200 nm was measured by a QCM close to the sample during the deposition. The substrates were at room temperature during the deposition, and the resulting film has an amorphous and porous morphology, which has been characterized by atomic force microscopy (Thrower et al. 2009).

The unit cell of the α-crystalline phase of methanol at 113 K, which contains two methanol molecules, has dimensions of $4.53 \times 4.69 \times 4.91$ Å (Sandford & Allamandola 1993). From these dimensions, values of $1.91 \times 10^{22}\,\mathrm{molecules\,cm^{-3}}$ and $7.16 \times 10^{14}\,\mathrm{molecules\,cm^{-2}}$ can be estimated for the bulk density, ρ_b, and surface density, ρ_s, respectively. Coverage is quoted in units of equivalent monolayers (ML_{eq}) where $1\,ML_{eq} = \rho_s$. Estimates of the thickness of the methanol layer are also made using these values, assuming a non-porous crystalline structure.

3 RESULTS AND DISCUSSION

Four sets of TPD traces for methanol desorption under varying conditions are shown in Fig. 1. Even a brief inspection of the four sets reveals that there are significant differences in behaviour.

Two peaks are evident for desorption of methanol from HOPG at lower coverages (Fig. 1A i). In the previous analysis of this data (BWB05), these peaks were attributed to interfacial (higher temperature peak) and amorphous multilayer (lower temperature peak) methanol desorptions. At higher coverages (Fig. 1A ii) the

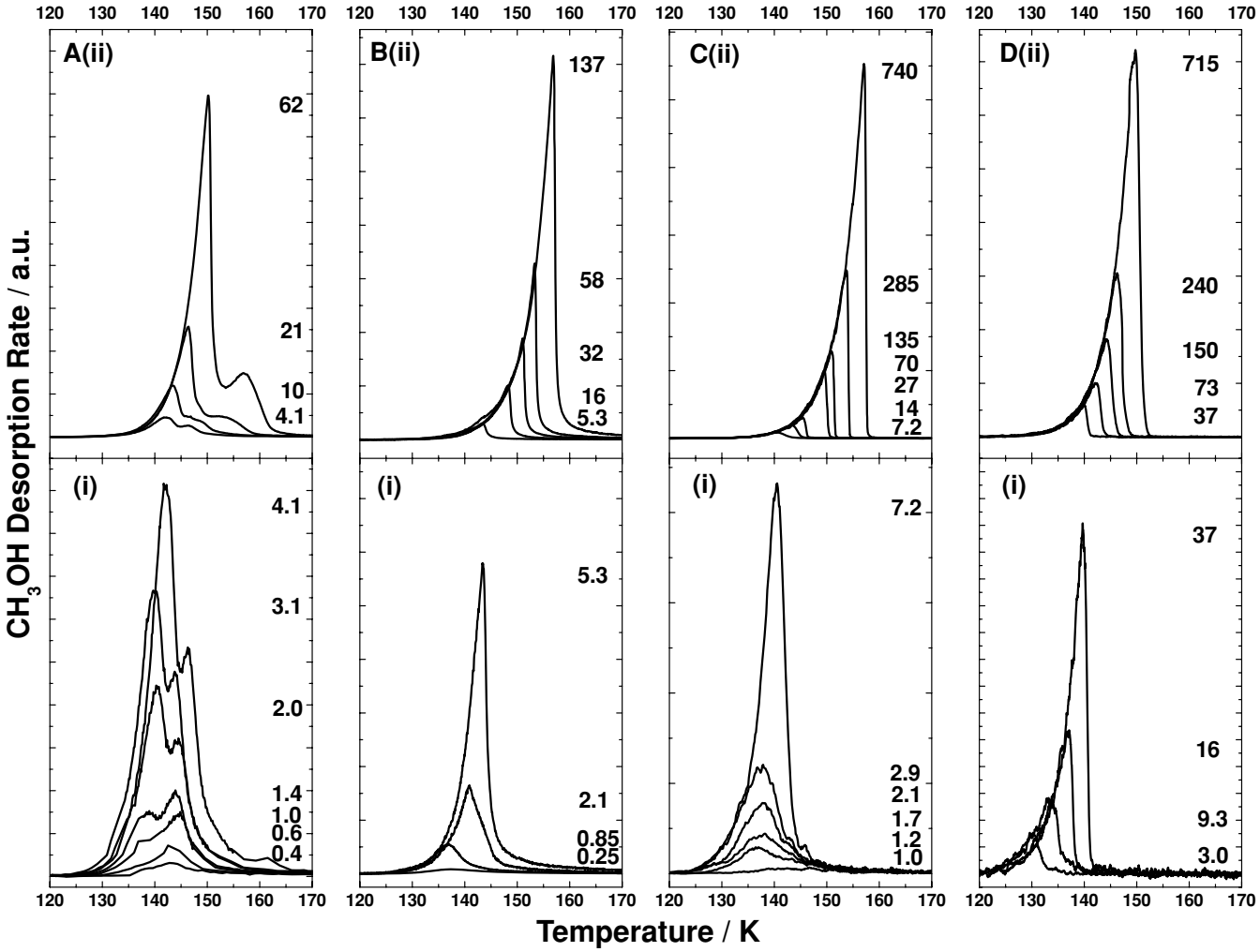

Figure 1. Experimental TPD profiles as a function of coverage, as indicated in ML_{eq}, for (i) lower coverages and (ii) higher coverages of solid methanol from (A) HOPG: chamber 1, deposition temperature = 89 K, $\beta = 0.5\,K\,s^{-1}$; (B) silica: chamber 3, deposition temperature = 118 K, $\beta = 0.1\,K\,s^{-1}$; (C) silica: chamber 2, deposition temperature = 19 K, $\beta \sim 0.1\,K\,s^{-1}$; (D) gold: chamber 2, deposition temperature = 18 K, $\beta \sim 0.03\,K\,s^{-1}$.

multilayer desorption peak dominates, however, there remain two well resolved desorption peaks. These were attributed to the desorptions of amorphous multilayer (lower temperature peak) and crystalline multilayer (higher temperature peak) methanol.

In contrast, in each of the three further data sets only a single methanol desorption peak is evident at all coverages (Figs 1B–D). At higher coverages, however, there is no evidence for distinct peaks due to amorphous and crystalline methanol. This is due to the difference in heating rates between these experiments and those shown in Fig. 1(A). At slower heating rates, the kinetics of crystallization dominate those of desorption of amorphous methanol. Indeed the infrared spectroscopy results originally presented with the TPD experiments in BWB05 reveal a substantially crystalline film following annealing to just 129 K for 3 min. At the higher temperature ramp in set A, however, the two processes compete, resulting in only partial crystallization, and desorption from both the amorphous and crystalline phases. The deposition temperature of 118 K for methanol on silica in set B is within the range reported for the onset of crystallization of amorphous methanol in various thin film studies (Peremans et al. 1990, 1994; Ayotte et al. 2002; BWB05) and well above that reported for bulk solid (Torrie, Weng & Powell 1989). Therefore, it is likely that a crystalline film is formed during deposition. However, deposition at 18 K, as for the experiments in Figs 1(C) and (D), should result in an amorphous methanol film (Bennett et al. 2007; Nagaoka, Watanabe & Kouchi 2007).

The rate of desorption of a species from a surface, r_{des} (molecules $cm^{-2}\,s^{-1}$), is given by the Polanyi–Wigner relationship (King 1975):

$$r_{des} = \nu_n N^n \exp\left(\frac{-E_{des}}{k_B T}\right), \quad (1)$$

where N is the coverage of the species (molecules cm^{-2}), T is the surface temperature (K), E_{des} is the desorption energy (J), k_B is the Boltzmann constant ($J\,K^{-1}$), n is the reaction order and ν_n is the nth order pre-exponential factor [(molecules $cm^{-2})^{1-n}\,s^{-1}$]. The order, desorption energy and pre-exponential factor are the kinetic parameters which define the desorption process for the species. In TPD experiments performed at a constant heating rate of $\beta(K\,s^{-1})$, a first-order desorption process, typical for a surface bound population of many species, is characterized by a maximum rate of desorption (i.e. the peak in the desorption trace) that is independent of coverage and gives rise to a slightly non-symmetrical peak shape. A zeroth-order process, typical for desorption of solid (multilayer) populations of

most species, is characterized by a highly non-symmetrical peak shape with a maximum that rises in temperature with increasing coverage. However, a series of TPD traces for different coverages of a zeroth-order desorption process will have coincident leading edges. The kinetic parameters can be extracted by analysis of the leading edge (King 1975). The Polanyi–Wigner relationship can be rewritten as

$$\ln\{r_{\rm des}\} = \ln\{\nu_n N^n\} - \frac{E_{\rm des}}{k_{\rm B}T}. \quad (2)$$

Therefore, from a series of TPD experiments with varying initial coverages, a plot of $\ln\{r_{\rm des}\}$ versus $\ln\{N\}$ for a fixed value of temperature, T, is linear with a gradient of n. Furthermore, a plot of $\ln\{r_{\rm des}\}$ versus $1/T$ for the leading edge of each desorption trace yields a straight line with a gradient of $-E_{\rm des}/k_{\rm B}$, and y-intercept of $n\ln\{\nu_n N_0\}$, where N_0 is the initial coverage. Therefore, values can be determined for the desorption energy and, providing n is known, the pre-exponential factor.

Kinetic parameters were previously determined for the interfacial and amorphous multilayer desorption peaks of methanol from HOPG using a leading edge analysis (BWB05). The desorption orders were found to be 1.23 ± 0.14 and 0.35 ± 0.21, respectively. Using these values, the desorption energies were both found to vary with coverage, increasing from 4000 to 5800 K (33–48 kJ mol^{-1}) for interfacial methanol and from 3700 to 4900 K (31–41 kJ mol^{-1}) for amorphous multilayer methanol. Kinetic parameters could not be determined for the crystalline multilayer desorption feature since the leading edge of the peak is never free from overlap with the amorphous desorption peak. Inspection of the peak shows that its maximum increases in temperature from roughly 147 to 157 K as the coverage increases from 10 to 62 ML$_{\rm eq}$, which would be consistent with a desorption order of close to zero. However, the more symmetrical shape of the peak is inconsistent with zeroth-order kinetics, and suggests greater complexity to this desorption step than can be determined from a simple analysis.

The interaction of methanol with the amorphous silica surface will be described in detail in a future publication. Briefly, however, at low coverages there is evidence of pore filling behaviour on the rough surface (not shown). This is in agreement with results recently obtained for benzene on this surface (Thrower et al. 2009), which indicate that the surface area of the amorphous silica is four to five times greater than its geometric surface area. For deposition at both 118 and 18 K, the methanol desorption appears to have fractional order up to a coverage of roughly 5 ML$_{\rm eq}$ (Figs 1B i and C i). At the higher coverages (Figs 1B ii and C ii) the coincident leading edges of the desorption traces and the shape of the desorption peaks are consistent with zeroth-order desorption. However, in the data set for methanol deposition at 118 K, the desorption profile for each coverage rises above the common leading edge in the last few degrees before the maximum (Fig. 1B i). This behaviour indicates that a more weakly adsorbed population of molecules, situated close to the substrate, is buried in the methanol film. The desorption profiles of higher coverages of methanol from the gold substrate (Fig. 1D ii) also show the common leading edge and shape consistent with zeroth-order kinetics. At lower coverages the desorption profiles retain the typical zeroth-order shape, but do not have coincident leading edges, which instead shift to higher temperatures with increasing coverage (Fig. 1D i).

It is clear that multiple desorption processes are simultaneously contributing to the leading edge of the desorption profile in data set B. This causes uncertainty in the interpretation of a $\ln(r_{\rm des})$ versus $\ln(N)$ plot in the leading edge analysis for desorption order. Furthermore, there are small discontinuities in the leading edge due to desorption from the heating wires. Therefore, it is only possible to conclude from such an analysis that the desorption at higher coverage is more or less consistent with zeroth-order kinetics. However, upon assuming zeroth-order desorption, the values determined for $E_{\rm des}$ and ν_0 with conservative error limits from a plot of $\ln(r_{\rm des})$ versus $1/T$ are 5200 ± 240 K (43.0 ± 2.0 kJ mol^{-1}) and $4.75 \times 10^{29\pm1}$ molecules cm^{-2} s^{-1}, respectively, for methanol deposited at high initial coverage (>5 ML$_{\rm eq}$) on silica at 118 K.

A constant heating rate is a requirement for the leading edge analysis. Since the heating rate was not constant throughout each TPD experiment performed in chamber 2, and varied slightly between experiments, leading edge analyses of the results for methanol deposited at low temperature on silica and gold (Figs 1C and D) are not possible. An alternative method of extracting kinetic parameters that we have previously applied involves fitting the desorption traces with simulations created using a stochastic integration package[1] (Fraser et al. 2001; Collings et al. 2003; Thrower et al. 2009). For a simple desorption process, a two-step simulation is created:

$$N_{\rm ice} \Rightarrow N_{\rm gas}, \quad (3)$$

$$N_{\rm gas} \Rightarrow N_{\rm pumped}, \quad (4)$$

where the rates of each reaction are given by

$$-\frac{{\rm d}N_{\rm ice}}{{\rm d}t} = \nu_n N_{\rm ice}^n \exp\left(\frac{-E_{\rm des}}{k_{\rm B}T}\right), \quad (5)$$

$$-\frac{{\rm d}N_{\rm gas}}{{\rm d}t} = \nu_{\rm pumped} N_{\rm gas}. \quad (6)$$

This method requires knowledge of the explicit surface coverage $N_{\rm ice}$ (molecules cm^{-2}). Furthermore, a value of the desorption order must be assumed, although inspection of the character of the desorption traces can provide insight into this value. The remaining unknown parameters, ν_n, $E_{\rm des}$ and $\nu_{\rm pump}$, can be varied iteratively until a good match to experimental results over a range of coverages is obtained. The position, width and shape of the desorption profiles provide sufficient parameter space to allow a unique fit to the experimental data. The advantages of this method include the ability to analyse data with non-linear temperature ramps, and the ability to combine multiple steps to analyse more complex desorption traces.

Comparisons of the higher coverage methanol desorptions from gold, and from silica at both deposition temperatures, with simulated profiles are shown in Figs 2(B)–(D). Good quality fits are obtained using a single zeroth-order desorption step, with values of $E_{\rm des}$ ranging from 5200 to 5465 K (43.0–45.45 kJ mol^{-1}), and a value of $3 \times 10^{30\pm1}$ molecules cm^{-2} s^{-1} for ν_0. The numerical results are summarized in Table 1, and compared to kinetic parameters determined for methanol desorption in other studies. In each data set the goodness of the fit is reduced for the lower coverages modelled, where the influence of desorption from the fractional order regime remains significant. The fractional order regime itself is too complex to simulate with a simple model in any of the sets. Both n and ν_n are likely to vary with coverage in this regime, making it impossible to obtain a unique fit using the simulation method of analysis.

Applying the previously determined kinetic parameters of BWB05 in a stochastic simulation of methanol desorption from

[1] CHEMICAL KINETICS SIMULATOR (CKS), Version 1.0, IBM Almaden Research Center, 650 Harry Road, Mailstop ZWX1D1, San Jose, CA, USA. Further information may be obtained from the CKS website at http://www.almaden.ibm.com/st/msim/ckspage.html.

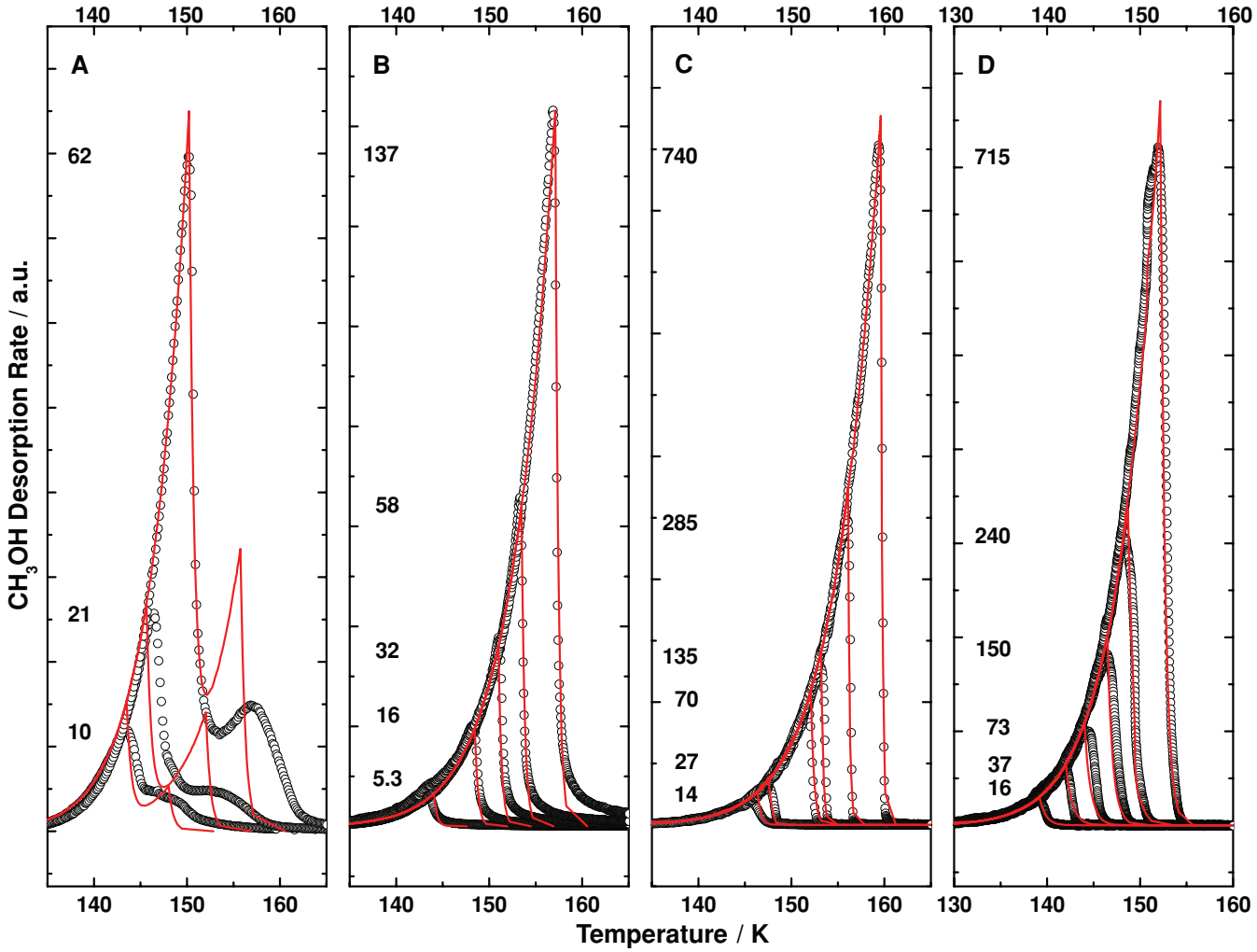

Figure 2. (Colour online) Comparison of experimental (black symbols) and simulated (red lines) TPD profiles as a function of coverage, as indicated in ML_{eq}, from (A) HOPG: chamber 1, deposition temperature = 89 K, $\beta = 0.5\,K\,s^{-1}$; simulation parameters: $E_{des} = 5470\,K$ and $\nu_0 = 2.5 \times 10^{31}$ molecules $cm^{-2}\,s^{-1}$ for the amorphous desorption (68 per cent of total); $E_{des} = 5470\,K$ and $\nu_0 = 3.0 \times 10^{30}$ molecules $cm^{-2}\,s^{-1}$ for the crystalline desorption (32 per cent of total), pump rate = $1\,s^{-1}$; (B) silica: chamber 3, deposition temperature = 118 K, $\beta = 0.5\,K\,s^{-1}$; simulation parameters: $E_{des} = 5465\,K$, $\nu_0 = 3 \times 10^{30}$ molecules $cm^{-2}\,s^{-1}$, pump rate = $0.1\,s^{-1}$; (C) silica: chamber 2, deposition temperature = 19 K, $\beta \sim 0.1\,K\,s^{-1}$; simulation parameters: $E_{des} = 5300\,K$, $\nu_0 = 3 \times 10^{30}$ molecules $cm^{-2}\,s^{-1}$, pump rate = $0.1\,s^{-1}$; (D) gold: chamber 2, deposition temperature = 18 K, $\beta \sim 0.03\,K\,s^{-1}$; simulation parameters: $E_{des} = 5200\,K$, $\nu_0 = 3 \times 10^{30}$ molecules $cm^{-2}\,s^{-1}$, pump rate = $0.03\,s^{-1}$.

HOPG failed to produce a satisfactory fit to the experimental data, with the simulated desorption being too broad and occurring at a substantially lower temperature than experiment. However, inspection of the experimental data suggests the amorphous peak may be approaching zeroth-order behaviour at the highest coverages. Fig. 2(A) compares the experimental results with simulated profiles of a two-step desorption process accounting for the amorphous and crystalline components of the desorption. A reasonable fit to the amorphous peak can be obtained with a zeroth-order model, although the fit is not as good as for the other substrates, since the fractional order contribution remains significant. On the other hand, the zeroth-order crystalline desorption step with the same kinetic parameters as the simulation of desorption from silica provides a very poor fit to the experimental data. The peak maxima of the simulated desorptions are at roughly the correct temperature, indicating some compatibility between experimental data sets, but the shape of the desorption demonstrates a complexity beyond that in the simple model applied in the simulation. Interestingly, if the lower temperature of the amorphous desorption was obtained by lowering E_{des} from the crystalline value, the resulting peak was far too broad. Rather, the fit was obtained by increasing ν_0, with E_{des} held at the crystalline value.

Fractional order desorption of multilayer methanol has been reported in several previous studies (Christmann & Demuth 1982; Wu et al. 1993; Nishimura et al. 1998; BWB05). Christmann & Demuth (1982) explained the fractional order of desorption by considering a condensed phase structure in which methanol forms chains of hydrogen-bonded molecules. The desorption energy of an end-chain molecule would be expected to be lower than that of a molecule in the middle of a chain since only one hydrogen bond must be broken. However, desorption of one mid-chain molecule would create two new end-chain molecules that are more easily desorbed. If the difference in desorption energy between the end-chain and mid-chain molecules is such that mid-chain desorption is significant but unfavoured, the desorption rate may be proportional to chain length and hence have fractional order with respect to the

Table 1. Kinetic parameters for desorption of solid methanol determined in varying experimental studies.

Substrate	β (K s^{-1})	Deposition temperature (K)	n (K)	$E_{\rm des}/k_{\rm B}$	ν_n
Gold[a]	∼0.03	18	0	5200 ± 120 $3 \times 10^{30\pm1}$	molecules cm^{-2} s^{-1}
Silica[a]	∼0.1	19	0	5300 ± 120 $3 \times 10^{30\pm1}$	molecules cm^{-2} s^{-1}
Silica[b] (simulation)	0.1	118	0	5465 ± 120 $3 \times 10^{30\pm1}$	molecules cm^{-2} s^{-1}
Silica[b] (leading edge)	0.1	118	0	5200 ± 240 $4.75 \times 10^{29\pm1}$	molecules cm^{-2} s^{-1}
HOPG[c,d,e] (Leading edge)	0.5	89	0.35 ± 0.21	4900 ± 100 6×10^{25}	(molecules cm^{-2})$^{0.65}$ s^{-1}
HOPG[f] (Simulation)	0.5	89	0	5470 ± 120 $2.5 \times 10^{31\pm1}$	molecules cm^{-2} s^{-1}
$Al_2O_3(0001)$[g]	5	90	0.53 ± 0.12	5580 ± 250 3.1×10^{24}	(molecules cm^{-2})$^{0.47}$ s^{-1}
CsI[h]	–	10	0	4230 ± 24 2.0×10^{27}	molecules cm^{-2} s^{-1}
Pd(100)[i]	12	77	0.5	3600	–
$\Delta H_{\rm sub}$ for bulk crystalline CH_3OH[g]				5390	

[a]This work, chamber 2.
[b]This work, chamber 3.
[c]BWB05.
[d]Bolina (2005).
[e]Brown & Bolina (2007).
[f]This work (analysis), chamber 1.
[g]Nishimura et al. (1998).
[h]Sandford & Allamandola (1993). These experiments measured desorption isothermally, therefore, the heating rate, β, is not applicable.
[i]Christmann & Demuth (1982).

total coverage. However, this model of fractional order desorption should be applicable on all surfaces, whereas zeroth-order desorption of multilayer methanol is also commonly observed. Nishimura et al. (1998) favoured a morphological explanation for fractional order desorption, in which the multilayer forms microstructures. The population of molecules available for desorption, and hence the desorption rate, is proportional to the surface area. Therefore, if microstructures form that have surface area which changes as the coverage is reduced during desorption, then the desorption rate will adopt a fractional order with respect to the coverage. Such islanding in the multilayer can occur when an adsorbate species does not wet the surface, i.e. when the adsorbate molecule binds more strongly to other adsorbate molecules than to the surface. Since methanol shows a different wetting character on each surface, this explanation can account for the observation of fractional order desorption kinetics on some surfaces but not others.

Methanol is not expected to wet the surface of HOPG (Wang et al. 2002). Therefore, formation of three-dimensional structures is a likely cause of the fractional order desorption from the amorphous phase. Methanol has been shown to wet the well defined (110) and (111) single crystal gold surfaces, forming a stable monolayer (Outka & Madix 1987; Gong et al. 2008). However, there is no evidence of a resolved monolayer desorption peak at higher temperature from the poorly defined and uncleaned polycrystalline gold film in these experiments (Fig. 1D i). At the low deposition temperature of 18 K in this experimental set, the adsorption is ballistic, i.e. the molecules are adsorbed where they collide with the surface, and have limited ability to relax into more energetically favourable configurations. The desorption profiles for coverages of less than 16 ML_{eq} are consistent with the process of dewetting, whereby the film restructures from this as-deposited morphology to increase interactions between adsorbate molecules and reduce the interactions between adsorbate molecules and the surface, and in so doing creates the microstructured surface from which fractional order desorption is observed. Dewetting is inhibited as the thickness increases (Palmer et al. 2008), therefore, at higher coverages the desorption is dominated by zeroth-order kinetics. At a deposition temperature of 89 K, it is likely that methanol is mobile on the HOPG surface (Souda 2005). Therefore, the film will dewet as it is deposited, allowing structuring at higher coverages than possible in a film that dewets as it anneals. Thus, the desorption profiles in data set A are not fully dominated by zeroth-order desorption even at the highest coverage of 62 ML_{eq}. Methanol is expected to wet the surface of silica (Sneh & George 1995). However, the intrinsic roughness of the amorphous silica substrate provides a three-dimensional surface upon which the surface area of the methanol film changes as it grows. Beyond a coverage of roughly 5 ML_{eq}, this surface roughness is effectively 'filled in' and zeroth-order desorption from layer-by-layer growth of the methanol film results.

The TPD experiment provides information about the adsorbate film in the temperature range during which desorption occurs, and cannot reliably give information about the thermal history of the film. It is therefore commonly assumed that the deposition temperature of the film is not important provided that it is below the start of significant desorption. Our interpretation of these results suggests, however, that due to the influence of effects such as dewetting, changes in deposition temperature may have measurable influences on the behaviour of the fractional order desorption regime. The deposition temperature may also have other, more subtle, effects. The structure and porosity of amorphous solid water is well known to be influenced by the temperature, rate and technique of deposition (Kimmel et al. 2001). A similar temperature dependency has been demonstrated in methanol films (Souda 2005; Collings, Chen & McCoustra 2006). Upon annealing, the structure of the film may not have the same structure as that of a film deposited at an equivalent temperature. This has also recently been demonstrated for ammonia films (Dawes et al. 2007). The influence of such effects is likely to be relatively small, and may be below the limit of sensitivity in many TPD experiments, but may nevertheless contribute to experimental uncertainty.

It is clear that methanol desorption shows a fractional order regime at relatively low coverages on each of the substrates examined, and that the behaviour of this regime is dependent on the substrate. However, it is also apparent that beyond this fractional order regime, a zeroth-order desorption regime grows. Comparison of the kinetic parameters in Table 1 shows that, as expected, there is no evidence to suggest that the structure of the methanol film is influenced by the substrate once this zeroth-order regime is

reached. Furthermore, the values of E_{des} obtained from desorption experiments are in good agreement with the value for the enthalpy of sublimation of bulk crystalline methanol estimated for an appropriate temperature (Nishimura et al. 1998). The values of E_{des} reported for methanol desorption from CsI (Sandford & Allamandola 1993) and Pd(100) (Christmann & Demuth 1982), however, are substantially lower. In the former case, E_{des} was calculated based on an estimated value of ν_0, and in the latter case no value of ν_0 was reported.

Because the desorption of methanol in the various studies has been performed under differing conditions, it is difficult to make direct graphical comparisons of the results. However, the stochastic simulation package can be used to generate methanol desorption profiles at a consistent set of 'experimental' conditions comparing differing sets of kinetic parameters. Fig. 3(A) compares simulations made using kinetic parameters determined for the four data sets (Figs 1A–D) and two additional sets from the literature (Sandford & Allamandola 1993; Nishimura et al. 1998). The four profiles with peaks in the 155 to 165 K range (Figs 3A i–iv) are due to desorption of crystalline methanol. The range of peak temperatures reflects uncertainties in the parameters. These uncertainties can arise from small errors in temperature calibration of experiments, and more significantly, from errors in measuring the coverage of adsorbed methanol, since the peak temperature for a zeroth-order desorption process is dependent on coverage. While the values of E_{des} and ν_0 reported by Sandford & Allamandola (1993) do differ from those determined in this work, in combination they produce a consistent desorption temperature. This demonstrates that the discrepancy in the parameters of Sandford & Allamandola (1993) arises in their calculation rather than the initial measurement of desorption rate.

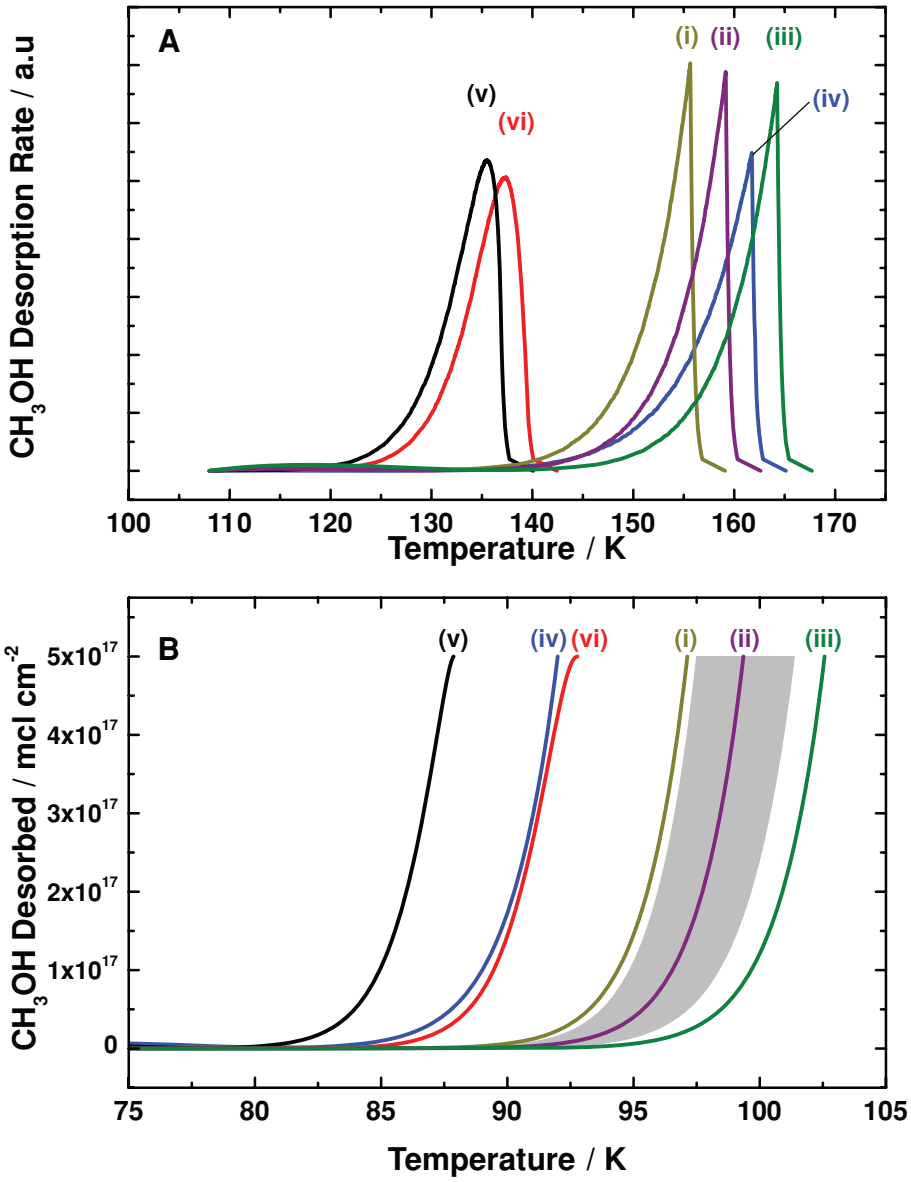

Figure 3. (Colour online) Simulated profiles of methanol desorption with various sets of experimentally measured kinetic parameters for a film of 5×10^{17} molecules cm^{-2} ($\sim$700 ML$_{eq}$) at (A) typical laboratory conditions of $\beta = 0.1$ K s^{-1} and a pump rate $= 0.3$ s^{-1}; and (B) with the temperature profile of a 15 M$_\odot$ protostar. Kinetic parameters for desorption from (i) gold, (ii) silica, deposition at 18 K and (iii) silica, deposition at 118 K from this work. The shaded region shows the range in temperature of the desorption profile in (ii) based on the experimental error. Kinetic parameters for desorption from (iv) CsI from Sandford & Allamandola (1993), (v) HOPG from BWB05 and (vi) Al_2O_3 from Nishimura et al. (1998).

The parameters determined for desorption of methanol from HOPG are known to relate to the amorphous phase, therefore, the peak occurs at a much lower temperature of 135 K in the simulated profile (Fig. 3A v), as expected. The peak in the simulated profile for methanol desorption from Al_2O_3 also occurs at a lower temperature (Fig. 3A vi). The authors assumed that the solid methanol was crystalline since the value of the desorption energy they determined was similar to the heat of sublimation of crystalline methanol. However, the desorption temperature and calculated value of $E_{\rm des}$ are consistent with amorphous desorption peak of from the graphite surface (Fig. 3A v). The higher heating rate employed in these experiments would also favour desorption from the amorphous state, as discussed below.

4 ASTROPHYSICAL APPLICATIONS

The results in Fig. 1(A) show that at a heating rate of 0.5 K s^{-1} the sublimation of solid methanol is dominated by desorption from the amorphous phase. However, in slowing the heating rate to 0.1 K s^{-1} or less, as in Figs 1(B)–(D), crystallization of the amorphous phase is complete prior to the onset of sublimation, so that only a single peak corresponding to the desorption of crystalline methanol is observed. Since the heating rate of icy mantles on dust grains close to protostars is many orders of magnitude slower, still it seems reasonable to assume that the desorption kinetics of amorphous methanol are unlikely to be of relevance in slowly warming circumstellar environments. However, this cannot be stated with certainty without a detailed knowledge of the kinetics of crystallization. The crystallization process consists of two components, the nucleation and the propagation of crystallites (Safarik & Mullins 2004). Nucleation can potentially be favoured in bulk ice, or at either the substrate or vacuum interface, which creates the possibility of the rate of crystallization having a dependence on ice thickness. In the case of water, the crystallization rate has been found to be satisfactorily approximated as a first order process (Kouchi et al. 1994). Water similarly shows a component of desorption from the amorphous phase at laboratory heating rates (for example Smith et al. 1997), but with the assumption of a first-order crystallization process, thermal desorption of water from the amorphous phase is not relevant at astrophysically relevant heating rates.

The temperature of thermal desorption of solid methanol under astrophysical conditions, such as in a warming nebula close to a protostar, can be determined by running the stochastic simulations with a temperature profile appropriate to the environment. In Fig. 3(B), desorption profiles simulated with the same six sets of kinetic parameters are compared, using the temperature profile of a 15 $M_\odot$ protostar (Viti et al. 2004). This temperature profile is in fact close to a linear heating rate of 2.6×10^{-3} K yr^{-1}. The pumping step in the simulation model has been removed so that the output of the simulation is a rise in the gas phase concentration of methanol. For the two profiles that simulate desorption of amorphous methanol (Figs 3B v and vi), the desorption again occurs at a markedly lower temperature. However, as discussed above, it is unlikely that thermal desorption occurs from the amorphous phase under astrophysically relevant conditions. The profile simulated for desorption of crystalline methanol from the parameters of Sandford & Allamandola (1993) shows desorption at a similarly low temperature. While the estimated value of ν_0 and the measured value of $E_{\rm des}$ based on this estimate can in combination be used to satisfactorily model desorption under laboratory conditions, at the astrophysically relevant heating rate they no longer give a reliable prediction of desorption temperature. The remaining three desorption profiles (Figs 3B i–iii) were obtained from the parameters determined for desorption of crystalline methanol in our own experiments. Even so, the uncertainties in our measurements allow for a variation in desorption temperature of up to 5 K.

Modelling the desorption of a solid film from a surface as a zeroth-order process assumes that the population of molecules available for desorption is constant over time. While this assumption may be valid for flat substrates under laboratory conditions, it is clearly not valid for three-dimensional substrates such as dust grain mantles, where surface area must decrease over time as the mantle contracts. The relationship describing a zeroth-order desorption process can hence be rewritten as

$$r_{\rm a} = \nu_0 A \, \exp\left(\frac{-E_{\rm des}}{k_{\rm B}T}\right), \tag{7}$$

where $r_{\rm a}$ (molecules s^{-1}) is the absolute desorption rate, and A (cm^2) is the time-dependent surface area from which molecules are desorbing. Substituting the basic equations describing the geometry of a sphere of radius l (cm),

$$A = 4\pi l^2, \tag{8}$$

$$V = \frac{4}{3}\pi l^3 = \frac{P}{\rho_{\rm b}}, \tag{9}$$

where V (cm^3) is the volume, P (molecules) is the number of molecules and $\rho_{\rm b}$ (molecules cm^{-3}) is the bulk molecular density, to obtain the expression

$$r_{\rm a} = 4.836\, \nu_0 \left(\frac{P}{\rho_{\rm b}}\right)^{2/3} \exp\left(\frac{-E_{\rm des}}{k_{\rm B}T}\right) \tag{10}$$

shows that a desorption process that is zeroth order on a flat sample has a fractional order with a value of 2/3 on a spherical particle. When the contribution of the volume of a grain of radius $l_{\rm g}$ (cm) to the dimensions of an icy mantle is taken into account, the rate expression becomes

$$r_{\rm a} = 12.57\, \nu_0 \left(0.2387\frac{P}{\rho_{\rm b}} + l_{\rm g}\right)^{2/3} \exp\left(\frac{-E_{\rm des}}{k_{\rm B}T}\right). \tag{11}$$

This is not an equation that can be solved using the stochastic integration package applied here. However, the profile of desorption from a mantle of uniform thickness adsorbed on a spherical grain is identical to that of a spherical icy ball of the same total dimensions, up until the point where the icy mantle is completely desorbed. Therefore, the expression in equation (10) is satisfactory for determining the desorption profiles of icy mantles from spherical grains, as has been done in the simulations described below.

The experimental results show that substrate-dependent fractional order methanol desorption is observed up to coverages of significance to mantle thicknesses on interstellar dust grains, due to the surface roughness. The effects of surface roughness in astrophysical environments are investigated in Fig. 4. Here, we crudely represent the rough surface as consisting of spherical 'granules'. The size of these granules is varied in order to mimic differences in the scale of the roughness. Desorption of an ice mantle from these granules therefore represents the fractional order desorption regime. The volume of methanol ice is the same for each simulation, and the thickness of the ice layer has been fixed at 50 nm (134 $ML_{\rm eq}$ on a flat surface), by varying the number of granules that contribute to the desorption profile. The parameter that changes between the simulations is the radius of curvature. For a granule of infinite diameter (i.e. a flat surface) the desorption profile is zeroth order, while for a granule of zero diameter (i.e. a spherical ball of ice) the desorption

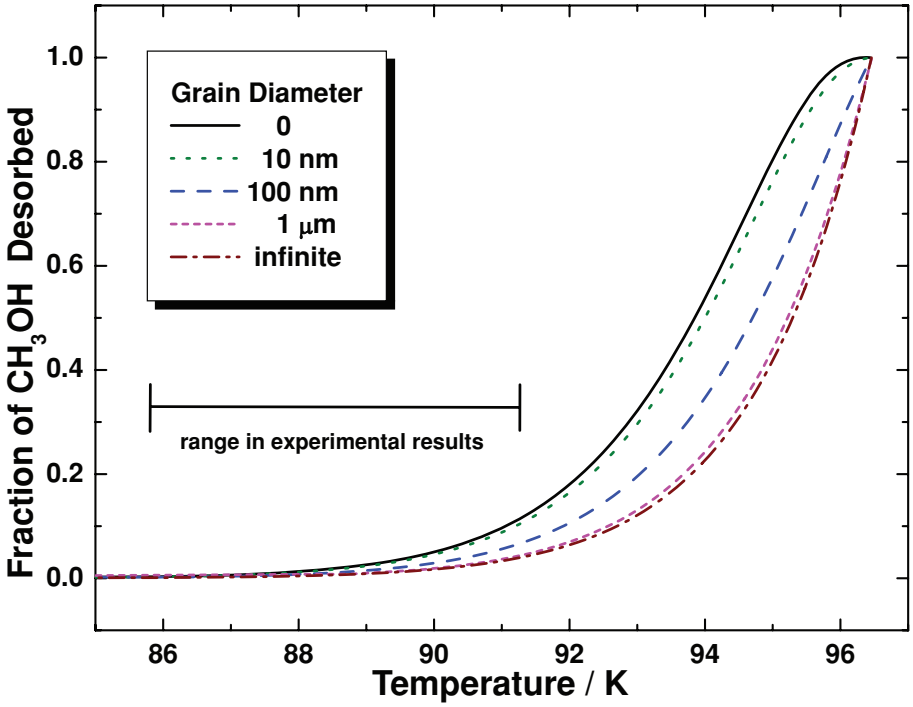

Figure 4. (Colour online) Simulated profiles for desorption of a fixed volume of methanol from spherical substrates with a range of diameters; the initial thickness of the methanol layer is fixed at 50 nm (assuming a bulk density of 1.91×10^{22} molecules cm^{-3}), with the number of spherical substrates varied such that the initial volume of methanol is equivalent. $E_{\rm des} = 5300$ K, $\nu_0 = 3 \times 10^{30}$ molecules cm^{-2} s^{-1}. The temperature profile of the 15 $M_\odot$ protostar is applied. The bar shows the 5 K range in desorption temperature from different sets of experimentally determined kinetic parameters (Figs 3B i–iii) for comparison.

profile has an order of 2/3. Using the same astrophysical temperature profile as applied in Fig. 3(B), the temperature difference between these two limiting cases is roughly 1.6 K at its maximum. The range of granule diameters applied represents a gross change in grain morphology. Therefore, the influence of surface roughness, in terms of the *shape* of the desorbing surface, has a relatively small effect on the desorption temperature under astrophysical conditions.

Fixing both the initial volume and thickness of methanol to constant values as the particle diameter is varied is actually an unphysical constraint, since the volume ratio of dust to ice (i.e. the column density ratio of refractory dust material to mantle material) must vary with particle diameter. In reality this ratio must be a fixed value in any particular environment, even if it is not precisely known. In Fig. 5, the influence of particle size is examined. Desorption profiles of a fixed volume of methanol are again compared as the particle diameter is varied, however, in this case, the volume ratio of the particle to the methanol ice mantle is fixed at a value of 3.0 by varying the number of dust particles which contribute to the methanol desorption. For a smooth spherical particle with a 1 μm diameter, this corresponds to a mantle thickness of 50 nm. As should be intuitively apparent, the initial thickness of methanol ice decreases with decreasing particle diameter. The desorption temperature of methanol falls by between 3 and 4 K for every order of magnitude of reduction in the particle diameter. The desorption rate is effectively increased for smaller particles due to the higher surface area available for desorption. This result is relevant when considering both the grain size and the roughness of the grain surface. In the first case, the grain itself is represented by a smooth spherical particle. This result demonstrates that under astrophysical conditions, grain *size* has a substantial influence on the desorption profile. In diffuse clouds, the grain population is known to vary approximately with grain size to the power of −3.5 (within a size range of 5–250 nm) (Tielens 2005). In dense clouds, and other environments where ice mantles are likely to accrete, the grain size distribution may vary from this law. However, the total volume of dust is dominated by the larger grains. Therefore, the ice volume and the desorption profile of the ice will be also be dominated by the larger grains. In the second case, the increased surface area is imparted by the decreased scale of the roughness. However, for larger grains the mantle thickness will be greater, therefore, it is more likely that the zeroth-order desorption regime will be reached, depending on the actual grain to mantle volume ratio in a particular environment.

The temperature profile of the 15 $M_\odot$ protostar was chosen for these simulations somewhat arbitrarily. The profile is of course an approximation, and treats the hot core for which it was developed as lacking spatial variation. We have previously investigated the influence of heating rate on the temperature of the thermal desorption of water and methanol (Collings et al. 2003; Brown & Bolina 2007) over the range from 1 K yr^{-1} to 1 K millennium^{-1}. The desorption temperatures vary by roughly 5 K per order of magnitude. Therefore, heating rate also has a large effect on the desorption temperature under astrophysical conditions.

5 CONCLUSIONS

The TPD of solid methanol from amorphous silica and gold substrates has been measured and compared to previously published data for desorption from a graphitic surface (BWB05). At lower coverages, the desorption shows substrate-dependent fractional order kinetics from each of these surfaces. However, on each surface, a zeroth-order desorption regime is reached when the coverage is sufficient. This threshold coverage is also substrate dependent, and we suggest that it is dependent on deposition temperature. Within the

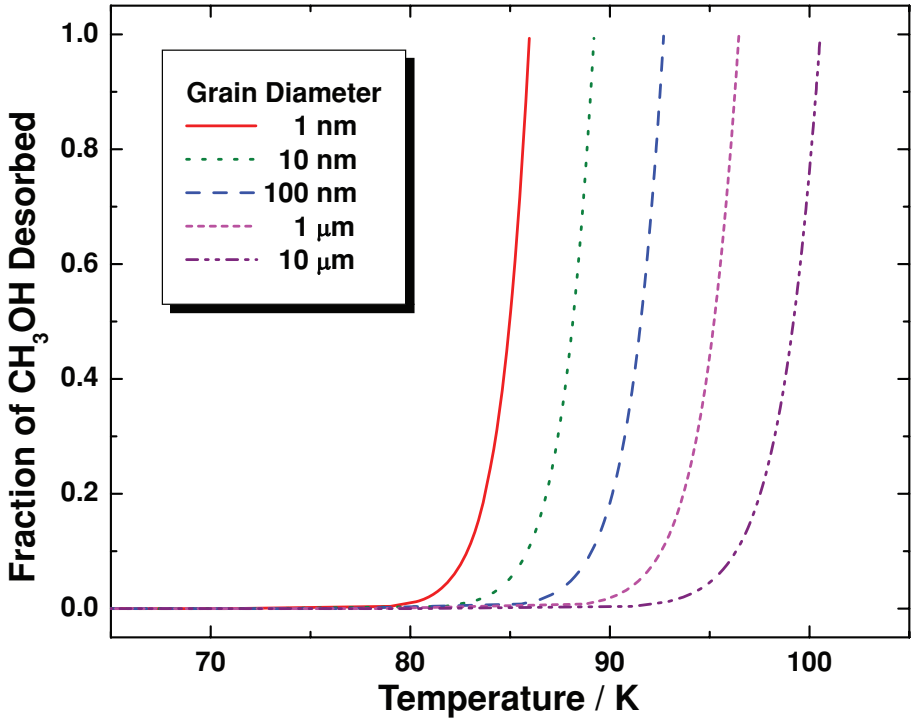

Figure 5. (Colour online) Simulated profiles for desorption of a fixed volume of methanol from spherical substrates with a range of diameters; the volume ratio of the substrate to methanol is fixed at 3.0, with the number of spherical substrates varied such that the initial volume of methanol is equivalent. $E_{\rm des}$ = 5300 K, $\nu_0 = 3 \times 10^{30}$ molecules cm^{-2} s^{-1}. The temperature profile of the 15 $M_\odot$ protostar is applied.

error limits of our measurements, the desorption in the zeroth-order regime is independent of the substrate, with a desorption energy of 5300 ± 180 K (44.0 ± 1.5 kJ mol^{-1}) and a pre-exponential factor of $10^{30\pm1.5}$ molecules cm^{-2} s^{-1}.

Using the experimentally measured kinetic parameters of the zeroth-order methanol desorption, models of methanol sublimation under astrophysically relevant conditions were created and used to investigate the influence of various factors on desorption temperature. The range in predicted desorption temperature due to these factors are

(i) 5 K due to uncertainty in the experimental measurements;
(ii) a maximum of 1.6 K due to changes in the particle shape;
(iii) 4 to 5 K per order of magnitude change in the heating rate;
(iv) 3 to 4 K per order of magnitude change in the diameter of a (spherical) dust particle.

Desorption of solid methanol in astrophysical environments is strongly dependent on the surface area from which it occurs, as determined by grain size and roughness, but less strongly influenced by the *shape* of the surface. This is likely to also be true of other species. Therefore, measurement of kinetic parameters in the zeroth-order desorption regime is sufficient to provide adequate models of the thermal desorption of solid species in astrophysical environments, and accurate kinetic analysis of the fractional order desorption regime will not necessarily advance this understanding. Furthermore, the desorption measurements can be made using any substrate, providing that the coverage is sufficient to ensure that zeroth-order desorption dominates. Of course, the nature of the substrate, in terms of both its composition and morphology, remains highly influential for the physicochemical behaviour of molecules in the interfacial layer. The precision of laboratory measurements of desorption kinetic parameters can and should be improved by further experimentation. However, the uncertainty and variation in astrophysical parameters, such as heating rate and dust grain size, remain the most limiting factors in precisely determining the temperature of thermal desorption of a species in astrophysical environments.

ACKNOWLEDGMENTS

The authors thank the participants of the 'Interstellar Surfaces: From Laboratory to Models' Workshop 2008, hosted by the Lorentz Center at the University of Leiden, the Netherlands, for useful discussions. The UCL and HWU groups both gratefully acknowledge the financial support of the Engineering and Physical Sciences Research Council (EPSRC), UK, in conducting this work. ASB and SDG acknowledge the support of EPSRC studentships, and RC acknowledges the support of an Overseas Research Student (ORS) Award, and additional funding from the University of Nottingham.

REFERENCES

Acharyya K., Fuchs G. W., Fraser H. J., van Dishoeck E. F., Linnartz H., 2007, A&A, 466, 1005
Attard G. A., Chilbane K., Ebert H. D., Parsons R., 1989, Surf. Sci., 224, 311
Ayotte P., Smith R. S., Teeter G., Dohnálek Z., Kimmel G. A., Kay B. D., 2002, Phys. Rev. Lett., 88, 245505
Bahr S., Toubin C., Kempter V., 2008, J. Chem. Phys., 128, 134712
Bennett C. J., Chen S.-H., Sun B.-J., Chang A. H. H., Kaiser R. I., 2007, ApJ, 660, 1588
Bolina A. S., 2005, PhD thesis, University College, London
Bolina A. S., Wolff A. J., Brown W. A., 2005, J. Chem. Phys., 122, 044713 (BWB05)
Brown W. A., Bolina A. S., 2007, MNRAS, 374, 1006

Brown W. A., Viti S., Wolff A. J., Bolina A. S., 2006, Faraday Discuss., 133, 113
Christmann K., Demuth J. E., 1982, J. Chem. Phys., 76, 6308
Collings M. P., Dever J. W., Fraser H. J., McCoustra M. R. S., 2003, Ap&SS, 286, 633
Collings M. P., Anderson M. A., Chen R., Dever J. W., Viti S., Williams D. A., McCoustra M. R. S., 2004, MNRAS, 354, 1133
Collings M. P., Chen R., McCoustra M. R. S., 2006, in Kaiser R. I., Bernath P., Osamura Y., Petrie S., Mebel A. M., eds, AIP Conf. Proc. Vol. 85, Astrochemistry: From Laboratory Studies to Astronomical Observations. Am. Inst. Phys., Melville, NY, p. 62
Dartois E., Schutte W., Geballe T. R., Demyk K., Ehrenfreund P., d'Hendecourt L., 1999, A&A, 342, L32
Dawes A. et al., 2007, J. Chem. Phys., 126, 244711
Fraser H. J., Collings M. P., McCoustra M. R. S., Williams D. A., 2001, MNRAS, 327, 1165
Fraser H. J., Collings M. P., McCoustra M. R. S., 2002, Rev. Sci. Instrum., 73, 2161
Gálvez O., Ortega I. K., Maté B., Moreno M. A., Martín-Llorente B., Herrero V. J., Escribano R., Gutiérrez P. J., 2007, A&A, 472, 691
Gong J., Flaherty D. W., Ojifinni R. A., White J. M., Mullins C. B., 2008, J. Phys. Chem. C, 112, 5501
Günster J., Liu G., Stultz J., Krischok S., Goodman D. W., 2000, J. Phys. Chem. B, 104, 5738
Harris T. D., Lee D. H., Blumberg M. Q., Arumainayagam C. R., 1995, J. Phys. Chem., 99, 9530
Herbst E., Shematovich V. I., 2003, Ap&SS, 285, 725
Hrbek J., dePaola R. A., Hoffmann F. M., 1984, J. Chem. Phys., 81, 2818
Jenniskens H. G., Dorlandt P. W. F., Kadodwala M. F., Kleyn A. W., 1996, Surf. Sci., 357, 624
Kimmel G. A., Stevenson K. P., Dohnálek Z., Smith R. S., Kay B. D., 2001, J. Chem. Phys., 114, 5284
King D. A., 1975, Surf. Sci., 47, 384
Kouchi A., Yamamoto T., Kozasa T., Kuroda T., Greenberg J. M., 1994, A&A, 290, 1009
Markwick A. J., Ilgner M., Millar T. J., Henning Th., 2002, A&A, 385, 632
Maté B., Gálvez O., Herrero V. J., Escribano R., 2009, ApJ, 690, 486
Nagaoka A., Watanabe N., Kouchi A., 2007, J. Phys. Chem. A, 111, 3016
Nishimura S. Y., Gibbons R. F., Tro N. J., 1998, J. Phys. Chem. B., 102, 6831
Oakes D. J., 1994, PhD thesis, Univ. East Anglia
Outka D. A., Madix R. J., 1987, J. Am. Chem. Soc., 109, 1708
Palmer J. S., Sivaramakrishnan S., Waggoner P. S., Weaver J. H., 2008, Surf. Sci., 602, 2278
Peremans A., Maseri F., Darville J., Gilles J.-M., 1990, J. Vac. Sci. Technol. A, 8, 3224
Peremans A., Dereux A., Maseri F., Darville J., Gilles J.-M., Vigneron J.-P., 1994, Phys. Rev. B, 45, 8598
Pontoppidan K. M., Dartois E., van Dishoeck E. F., Thi W.-F., d'Hendecourt L., 2003, A&A, 404, L17
Pontoppidan K. M., van Dishoeck E. F., Dartois E., 2004, A&A, 426, 925
Pratt S. J., Escott D. K., King D. A., 2003, J. Chem. Phys., 19, 10867
Rendulic K. D., Sexton B. A., 1982, J. Catal., 78, 126
Roberts J. F., Rawlings J. M. C., Viti S., Williams D. A., 2007, MNRAS, 382, 733
Safarik D. J., Mullins C. B., 2004, J. Chem. Phys., 121, 6003
Sandford S. A., Allamandola L. J., 1993, ApJ, 417, 815
Sexton B. A., 1981, Surf. Sci., 102, 271
Sexton B. A., Hughes A. E., 1984, Surf. Sci., 140, 227
Sexton B. A., Rendulic K. D., Hughes A. E., 1982, Surf. Sci., 121, 181
Smith R. S., Huang C., Wong E. K. L., Kay B. D., 1997, Phys. Rev. Lett., 79, 909
Sneh O., George S. M., 1995, J. Phys. Chem., 99, 4639
Souda R., 2005, Phys. Rev. B, 72, 115414
Thrower J. D., Collings M. P., Rutten F. J. M., McCoustra M. R. S., 2009, MNRAS, 354, 1510
Tielens A. G. G. M., 2005, The Physics and Chemistry of the Interstellar Medium. Cambridge Univ. Press, Cambridge
Tielens A. G. G. M., Whittet D. C., 1997, in van Dishoeck E. F., ed., Molecules in Astrophysics. Kluwer, Dordrecht, p. 239
Torrie B. H., Weng S. X., Powell B. M., 1989, Mol. Phys., 67, 575
Viti S., Williams D. A., 1999, MNRAS, 305, 755
Viti S., Collings M. P., Dever J. W., McCoustra M. R. S., Williams D. A., 2004, MNRAS, 354, 1141
Wang L., Song Y., Wu A., Li Z., Zhang B., Wang E., 2002, Appl. Surf. Sci., 199, 67
Watanabe N., Kouchi A., 2008, Prog. Surf. Sci., 83, 439
Wolff A. J., Carlstedt C., Brown W. A., 2007, J. Phys. Chem. C., 111, 5990
Woodruff D. P., Delcher T. A., 1994, Modern Techniques of Surface Science, 2nd edn. Cambridge Univ. Press, Cambridge
Wu M.-C., Truong C. M., Goodman D. W., 1993, J. Phys. Chem., 97, 9425
Zhang R., Gellman A. J., 1991, J. Phys. Chem., 95, 7433

This paper has been typeset from a MS Word file perpared by the author.